

Peptide nucleic acids (PNA) derived from *N*-(*N*-methylaminoethyl)glycine. Synthesis, hybridization and structural properties§

Gerald Haaima,^{†a} Hanne Rasmussen,^b Günther Schmidt,^a Dorte K. Jensen,^a
Jette Sandholm Kastrup,^b Pernilla Wittung Stafshede,^{‡c} Bengt Nordén,^c
(the late) Ole Buchardt^a and Peter E. Nielsen^{*d}

^a Center for Biomolecular Recognition, The H. C. Ørsted Institute, Universitetsparken 5, DK-2100 Ø, Copenhagen, Denmark

^b Department of Medicinal Chemistry, Royal Danish School of Pharmacy, Universitetsparken 2, DK-2100 Ø, Copenhagen, Denmark

^c Department of Physical Chemistry, Chalmers University of Technology, S-41296, Gothenburg, Sweden

^d Center for Biomolecular Recognition, Department of Biochemistry and Genetics, Laboratory B, The Panum Institute, Blegdamsvej 3c, DK-2200 N, Copenhagen, Denmark.
E-mail: pen@imbg.ku.dk

Received (in Cambridge, UK) 15th March 1999, Accepted 24th May 1999

Backbone *N*-methylated peptide nucleic acids (PNAs) containing the four nucleobases adenine, cytosine, guanine and thymine were synthesized *via* solid phase peptide oligomerization. The oligomers bind to their complementary target with a thermal stability that is 1.5–4.5 °C lower per “*N*-methyl nucleobase unit” [dependent on the number and position(s) of the *N*-methyl] than that of unmodified PNA. However, even fully *N*-methyl modified PNAs bind as efficiently to DNA or RNA targets as DNA itself. Furthermore, the hybridization efficiency per *N*-methyl unit in a PNA decreased with increasing *N*-methyl content, and the effect was more pronounced when the *N*-methyl backbone units are present in the Hoogsteen *versus* the Watson–Crick strand in (PNA)₂-DNA triplexes. Interestingly, CD spectral analyses indicate that 30% (3 out of ten) substitution with *N*-methyl nucleobases did not alter the structure of PNA-DNA (or RNA) duplexes or (PNA)₂-DNA triplexes, and likewise CD spectroscopy and X-ray crystallography showed no major structural differences between *N*-methylated (30%) and unmodified PNA-PNA duplexes. However, PNA-DNA duplexes as well as triplexes adopted a different conformation when formed with all-*N*-methyl PNAs.

Introduction

Reagents that interact with DNA or RNA in a sequence specific manner are of great interest for the development of gene therapeutic drugs and diagnostic and molecular biology tools.^{1–3} Peptide nucleic acid (PNA) is a DNA mimic in which the sugar-phosphate backbone is replaced by a backbone consisting of *N*-(2-aminoethyl)glycine units.^{4–6} The chemical, biophysical and biological properties of PNA, not least the finding that PNA oligomers hybridize strongly and sequence specifically to complementary DNA, RNA or PNA oligomers, have attracted attention towards this and analogous peptide nucleic acids.^{7–12} A significant number of PNA derivatives with modifications in the backbone have been prepared and are currently being studied in order to understand the chemi-

cal and structural features which are important for nucleic acid binding and recognition as well as biological activity.^{11–24}

In order to further investigate the structure–activity relationships of PNA, a modified PNA backbone, which contains an *N*-(2-methylaminoethyl)glycine was considered. This substitution eliminates the hydrogen bonding donor capacity of the backbone as well as changes the hydrophilicity and hydration properties. It has been proposed on the basis of molecular modeling that the carbonyl of the linker to the nucleobase constitutes a potential hydrogen bonding acceptor for this amide proton, either in the direction of the amide NH of the same or to the preceding nucleobase unit.^{25,26} However, neither NMR^{27,28} nor X-ray crystallographic²⁹ three-dimensional structure determinations of PNA-DNA/RNA/PNA duplexes or a (PNA)₂-DNA triplex have supported such a hydrogen bonding pattern. In fact, the crystal structures show that the backbone amide protons of the Hoogsteen PNA strand in the (PNA)₂-DNA triplex are involved in specific hydrogen bonds to the phosphates of the DNA backbone,²⁹ whereas the backbone amide protons in the PNA-PNA duplex are hydrogen bonded to localized water molecules which bridge the nucleobase and the backbone.³⁰

In this paper we report the synthesis and hybridization

[†] Present address: Center for Drug Design and Development, University of Queensland, Brisbane QLD 4072, Australia.

[‡] Present address: Beckman Institute, California Institute of Technology, Pasadena, 91125 California, USA.

§ Abbreviations used: DCC dicyclohexylcarbodiimide; DCU dicyclohexyl urea; DhbtOH 3,4-dihydro-3-hydroxy-4-oxo-1,2,3-benzotriazine; HATU *O*-(7-azabenzotriazol-1-yl)-1,1,3,3-tetramethyluronium hexafluorophosphate.

analysis of PNA oligomers containing *N*-methylated glycine units at one or more positions along the backbone. Furthermore, the effect of backbone *N*-methylation on the structure of PNA complexes has been investigated by CD spectroscopy and X-ray crystallography.

Experimental

General

All reagents were obtained from commercial suppliers and used without further purification. Melting points are uncorrected. Flash chromatography was performed using Merck silica gel 60 (230–400 mesh ASTM). ^1H and ^{13}C NMR spectra were obtained in DMSO- d_6 using a Varian 400 MHz Unity or a Bruker 250 MHz AMX spectrometer. Fast atom bombardment mass spectra were recorded on a JEOL Hx110/110 operating in positive ion mode. MALDI-TOF mass spectra of PNA oligomers were recorded on a Kratos, Kompact Maldi II operating in positive ion mode and using 3,5-dimethoxy-4-hydroxycinnamic acid as the matrix.

Analytical HPLC was carried out on a 3.9×150 mm Delta Pak 5 μm C-18 100 Å column (Waters). Buffer A: 99.9% H_2O –0.1% TFA; Buffer B: 10% H_2O –89.9% CH_3CN –0.1% trifluoroacetic acid (TFA). The solvents were heated to 50°C while the flow rates were 1.0 for analytical and 2.0 ml min^{-1} for preparative HPLC.

RNA oligomers were purchased from DNA Technology, Aarhus, Denmark and were used as received, and DNA oligomers were synthesized by standard methods. Thermal denaturation studies (T_m) were run on a Gilford Response II spectrophotometer scanning from 5 to 90°C at a rate of 0.5°C per step (approx. $0.7^\circ\text{C min}^{-1}$). Prior to recording the T_m , the complexes were heated to 95°C for 5 min and allowed to slowly cool to 4°C . The oligomers were hybridized in the following buffer: 100 mM NaCl–10 mM sodium phosphate–0.1 mM H_4EDTA , pH 7.0. The concentrations of PNA and oligonucleotides were determined optically at 60°C using the molar absorptivities of the four nucleosides.

CD spectra were recorded on a Jasco model 720 spectropolarimeter equipped with a thermoelectrically controlled cell holder. Each spectrum is the average of at least eight scans, recorded at 20°C using 1 cm optical path length. The samples were kept in a 5 mM sodium phosphate buffer at pH 7.0.

Monomer synthesis

***N*-Methyl-1-aminopropane-2,3-diol 1.** To a pre-cooled solution (0°C) of methylamine (172 ml of a 40% solution in water, 2 mol) was added 2,3-epoxypropan-1-ol (25 g, 0.34 mol) at such a rate that the reaction temperature did not exceed 10°C . After 3 h at 0°C excess methylamine and water were evaporated and the residue Kugelrohr distilled (103 – 105°C , 0.5 mmHg) resulting in 25.6 g (76%) of colorless oil. ^1H NMR (400 MHz, CDCl_3): δ 3.74 (m, 1H, CH), 3.56 (m, 2H, CH_2), 3.22 (m, 2H, CH_2), 2.94 (s, 3H, NCH_3); FAB-MS: m/z 106 ($\text{M}^+ + \text{H}$).

1-[*N*-(*tert*-Butyloxycarbonyl)-*N*-methyl]aminopropane-2,3-diol 2. Di-*tert*-butyl dicarbonate (52.3 g, 0.24 mol) was added to a pre-cooled (0°C) solution of **1** (21 g, 0.20 mol) in water (340 ml) and the mixture was allowed to warm to room temperature. The pH was maintained at 10.5 by addition of 4 M aqueous NaOH. After addition of 2 equivalents of NaOH the reaction was left to stir for 15 h. Upon cooling to 0°C and adjusting the pH to 2.5 using 4 M aqueous HCl the reaction mixture was extracted with EtOAc (6×100 ml). The combined organic fractions were washed with half-saturated aqueous KHSO_4 (3×150 ml) followed by brine (1×150 ml). The organic fraction was then dried (MgSO_4) and concentrated to an oil. Kugelrohr distillation (110 – 112°C , 0.5

mmHg) furnished 31.3 g (81%) of the desired product as a colorless oil. ^1H NMR (400 MHz, CDCl_3): δ 3.72 (m, 1H, CH), 3.55 (m, 2H, CH_2), 3.22 (m, 2H, CH_2), 2.90 (s, 3H, NCH_3), 1.43 (s, 9H, *t*-Bu); FAB-MS: m/z 206 ($\text{M}^+ + \text{H}$).

2-{[*N*-(*tert*-Butyloxycarbonyl)-*N*-methyl]amino}acetaldehyde 3. To a solution of **2** (20 g, 97 mmol) in water (100 ml) stirring under N_2 was added KIO_4 (24.68 g, 108 mmol). After 2.5 h the reaction mixture was filtered and the filtrate extracted with CHCl_3 (5×50 ml). The CHCl_3 layers were dried (MgSO_4) and concentrated to an oil. Kugelrohr distillation (76 – 80°C , 0.5 mmHg) provided 13.26 g (79%) of a colorless oil. ^1H NMR (400 MHz, CDCl_3): δ 8.54 (s, 1H, major, CHO), 8.51 (s, 1H, minor, CHO), 4.01 (s, 2H, major, CH_2), 3.93 (s, 2H, minor, CH_2), 2.95 (s, 3H, major, NCH_3), 2.93 (s, 3H, minor, NCH_3), 1.47 (s, 9H, major, *t*-Bu); 1.42 (s, 9H, minor, *t*-Bu); FAB-MS: m/z 174 ($\text{M}^+ + \text{H}$).

Ethyl *N*-{2-[(*N*-*tert*-butyloxycarbonyl)-*N*-methyl]aminoethyl}glycinate 4. Ethyl glycinate hydrochloride (8.10 g, 58 mmol) dissolved in absolute EtOH (100 ml) was added dropwise to a cooled (0°C) solution of **3** (10.0 g, 58 mmol) and NaOAc (9.32 g, 114 mmol) in absolute EtOH (130 ml). After addition of 10% Pd on carbon (1.65 g) the reaction was hydrogenated (1 atm) until one equivalent of H_2 was absorbed. The reaction mixture was filtered and to the filtrate was added water (80 ml). After adjusting the pH to 8 with 2 M aqueous NaOH the mixture was extracted with CH_2Cl_2 (5×60 ml). The organic layers were dried (MgSO_4) and concentrated to an oil. Kugelrohr distillation (100 – 105°C , 0.5 mmHg) furnished 10.6 g (74.3%) of a colorless oil. ^1H NMR (250 MHz, CDCl_3): δ 4.18 (q, 2H, CH_2), 3.42 (s, 2H, CH_2), 3.34 (t, 2H, CH_2), 2.88 (s, 3H, CH_3), 2.77 (t, 2H, CH_2), 1.45 (s, 9H, *t*-Bu), 1.28 (t, 3H, CH_3); FAB-MS: m/z 261 ($\text{M}^+ + \text{H}$).

General procedure for the synthesis of the monomer esters 5a–d

To a pre-cooled (0°C) solution of **4** (7.0 mmol), DhbtOH (7.7 mmol) and the appropriate carboxymethyl derivative of the nucleobase (7.7 mmol) in a 1:1 mixture of dry DMF– CH_2Cl_2 (60 ml) was added DCC (8.4 mmol). After stirring at 0°C for 1 h followed by a further 3 h at room temperature the precipitated DCU was removed by filtration and the reaction work-up was as follows for each derivative.

Ethyl *N*-{2-[(*N*-*tert*-butyloxycarbonyl)-*N*-methyl]aminoethyl}-*N*-[(thymine-1-yl)acetyl]glycinate 5a. The reaction was diluted with CH_2Cl_2 (60 ml) and washed sequentially with half-saturated aqueous NaHCO_3 (3×30 ml), half-saturated aqueous KHSO_4 (2×30 ml) and brine (1×30 ml). The organic phase was dried (MgSO_4) and the solvent removed *in vacuo*. The resulting foam was redissolved in CH_2Cl_2 , cooled to 0°C and precipitated by slow addition of light petroleum (bp 40 – 60°C) under vigorous stirring. The product was isolated as a white solid; mp 93 – 95°C ; ^1H NMR (400 MHz, CDCl_3): δ 11.20 (s, 1H, major, T-imid NH), 11.18 (s, 1H, minor, T-imid NH), 7.52 (s, 1H, major, T-H6), 7.50 (s, 1H, minor, T-H6), 4.60 (s, 2H, major, CH_2CON), 4.42 (s, 2H, minor, CH_2CON), 4.32 (q, 2H, OCH_2CH_3), 4.25 (s, 2H, minor, CH_2COOH), 4.07 (s, 2H, major, CH_2COOH), 3.60–3.10 (m, CH_2CH_2), 2.90 (s, 3H, major, BocNCH_3), 2.83 (s, 3H, minor, BocNCH_3), 1.79 (s, 3H, CH_3), 1.39 (s, 9H, *t*-Bu), 1.34 (t, 3H, OCH_2CH_3); FAB-MS: m/z 427 ($\text{M}^+ + \text{H}$).

Ethyl *N*-{2-[(*N*-*tert*-butyloxycarbonyl)-*N*-methyl]aminoethyl}-*N*-{[4-*N*-(benzyloxycarbonyl)cytosine-1-yl]acetyl}glycinate 5b. The reaction mixture was evaporated to dryness and to the residue was added diethyl ether (50 ml), this was stirred for 2 h and the solid filtered off. The solid was again stirred with 50 ml ether for 2 h and filtered off, washing the solid with half-saturated aqueous NaHCO_3 . The solid was then dissolved in hot dioxane (60 ml) and precipitated by slow addition of water (60 ml). The product was further purified by

column chromatography (SiO₂, MeOH–CH₂Cl₂, 5 : 95); mp 152–156 °C; ¹H NMR (400 MHz, CDCl₃): δ 7.98 (s, 1H, C-H5), 7.42–7.34 (m, 5H, Ph), 7.09 (s, 1H, C-H6), 5.19 (s, 2H, PhCH₂), 4.85 (s, 2H, major, CH₂CON), 4.62 (s, 2H, minor, CH₂CON), 4.28 (q, 2H, OCH₂CH₃), 4.17 (s, 2H, minor, CH₂COOH), 3.99 (s, 2H, major, CH₂COOH), 3.42–3.03 (m, CH₂CH₂), 2.97 (s, 3H, major, BocNCH₃), 2.89 (s, 3H, minor, BocNCH₃), 1.39 (s, 9H, *t*-Bu), 1.24 (t, 3H, OCH₂CH₃); FAB-MS: *m/z* 546 (M⁺ + H).

Ethyl *N*-{2-[(*N*-*tert*-butyloxycarbonyl)-*N*-methyl]aminoethyl}-*N*-{[6-*N*-(benzyloxycarbonyl)adenin-9-yl]acetyl}-glycinate 5c. The reaction mixture was evaporated to dryness, redissolved in CH₂Cl₂ (300 ml) and washed successively with half-saturated aqueous NaHCO₃ (3 × 100 ml), half-saturated aqueous KHSO₄ (2 × 100 ml) and brine (1 × 100 ml). The organic phase was dried (MgSO₄) and the solvent removed *in vacuo*. To the resulting foam in absolute EtOH (60 ml) was slowly added water (30 ml). The mixture was left stirring overnight and the product was isolated by filtration; mp 140–143 °C; ¹H NMR (400 MHz, CDCl₃): δ 9.19 (br s, 1H, ZNH), 8.74 (s, 1H, major, H-8), 8.06 (s, 1H, minor, H-8), 7.47–7.32 (m, 5H, Ph), 5.29 (s, 2H, major, CH₂CON), 5.14 (s, 2H, minor, CH₂CON), 5.24 (s, 2H, PhCH₂), 4.27 (s, 2H, minor, CH₂COOH), 4.17 (q, 2H, OCH₂CH₃), 4.02 (s, 2H, major, CH₂COOH); 3.54–3.03 (m, CH₂CH₂), 2.93 (s, 3H, major, BocNCH₃), 2.86 (s, 3H, minor, BocNCH₃), 1.40 (s, 9H, *t*-Bu), 1.26 (t, 3H, OCH₂CH₃); FAB-MS: *m/z* 570 (M⁺ + H).

Ethyl *N*-{2-[(*N*-*tert*-butyloxycarbonyl)-*N*-methyl]aminoethyl}-*N*-{[6-*N*-(benzyloxycarbonyl)guanin-9-yl]acetyl}-glycinate 5d. The reaction mixture was evaporated to dryness, redissolved in CH₂Cl₂ (80 ml) and washed with half-saturated aqueous KHSO₄ (3 × 40 ml). After drying (MgSO₄) and removal of the solvent *in vacuo* the desired product was isolated by crystallization from EtOAc; mp 157–159 °C; ¹H NMR (400 MHz, CDCl₃): δ 7.95 (s, 1H, major, G-H8), 7.88 (s, 1H, minor, G-H8), 7.55–7.38 (m, 5H, Ph), 5.37 (s, 2H, PhCH₂), 5.18 (s, 2H, major, CH₂CON), 5.00 (s, 2H, minor, CH₂CON), 4.36 (s, 2H, minor, CH₂COOH), 4.20 (q, 2H, OCH₂CH₃), 4.06 (s, 2H, major, CH₂COOH), 3.62–3.32 (m, CH₂CH₂), 2.94 (s, 3H, major, BocNCH₃), 2.80 (s, 3H, minor, BocNCH₃), 1.38 (s, 9H, *t*-Bu), 1.27 (t, 3H, OCH₂CH₃); FAB-MS: *m/z* 586 (M⁺ + H).

***N*-{2-[(*N*-*tert*-Butyloxycarbonyl)-*N*-methyl]aminoethyl}-*N*-[(thymine-1-yl)acetyl]glycine 6a.** To a solution of 5a (2.41 g, 5.6 mmol) in MeOH (45 ml) at 0 °C was added 2 M NaOH (45 ml) and stirring was continued for 2 h. The pH was adjusted to 2 with 2 M HCl and extracted with ethyl acetate. The organic phase was dried (MgSO₄) and evaporated to dryness yielding 1.45 g (52%) of a white solid; mp 119–122 °C; ¹H NMR (400 MHz, DMSO-*d*₆): δ 12.83 (s, 1H, COOH), 11.36 (s, 1H, major, T-imid NH), 11.34 (s, 1H, minor, T-imid NH), 7.38 (s, 1H, major, T-H6), 7.34 (s, 1H, minor, T-H6), 4.72 (s, 2H, major, CH₂CON), 4.54 (s, 2H, minor, CH₂CON), 4.26 (s, 2H, minor, CH₂COOH), 4.04 (s, 2H, major, CH₂COOH), 3.70–3.10 (m, CH₂CH₂), 2.92 (s, 3H, major, BocNCH₃), 2.84 (s, 3H, minor, BocNCH₃), 1.75 (s, 3H, CH₃), 1.38 (s, 9H, *t*-Bu); FAB-MS: *m/z* 399 (M⁺ + H); Calc. for C₁₇H₂₆N₄O₇: C, 51.25; H, 6.58; N, 14.07. Found: C, 50.98; H, 6.55; N, 13.90%.

***N*-{2-[(*N*-*tert*-Butyloxycarbonyl)-*N*-methyl]aminoethyl}-*N*-{[4-*N*-(benzyloxycarbonyl)cytosin-1-yl]acetyl}glycine 6b.** To a solution of 5b (1.17 g, 2.3 mmol) in THF (40 ml) was added 1 M aqueous LiOH (60 ml). After 30 min the reaction was cooled to 0 °C and the pH was adjusted to 2 with 2 N aqueous HCl. The mixture was extracted with CH₂Cl₂ and the organic phase was dried (MgSO₄) and evaporated yielding

0.72 g (27%) of white foam; mp 181–184 °C; ¹H NMR (400 MHz, DMSO-*d*₆): δ 10.78 (s, 1H, COOH), 7.88 (s, 1H, C-H5), 7.41–7.32 (m, 5H, Ph), 7.01 (s, 1H, C-H6), 5.19 (s, 2H, PhCH₂), 4.81 (s, 2H, major, CH₂CON), 4.62 (s, 2H, minor, CH₂CON), 4.17 (s, 2H, minor, CH₂COOH), 3.98 (s, 2H, major, CH₂COOH), 3.42–3.03 (m, CH₂CH₂), 2.94 (s, 3H, major, BocNCH₃), 2.87 (s, 3H, minor, BocNCH₃), 1.38 (s, 9H, *t*-Bu); FAB-MS: *m/z* 518 (M⁺ + H); Calc. for C₂₄H₃₁N₅O₈: C, 55.69; H, 6.04; N, 13.53. Found: C, 55.35; H, 5.99; N, 13.28%.

***N*-{2-[(*N*-*tert*-Butyloxycarbonyl)-*N*-methyl]aminoethyl}-*N*-{[6-*N*-(benzyloxycarbonyl)adenin-9-yl]acetyl}glycine 6c.** To a solution of 5c (3.14 g, 5.5 mmol) in THF at 0 °C was added 1 N aqueous LiOH (25 ml). After 30 min the pH was adjusted to 1 with 2 N aqueous HCl. The precipitate was filtered and dried yielding 1.62 g (57%) of a white solid; mp 171–173 °C; ¹H NMR (400 MHz, DMSO-*d*₆): δ 12.77 (broad, 1H, COOH), 10.68 (broad, 1H, ZNH), 8.59 (s, 1H, major, A-H8), 8.35 (s, 1H, minor, A-H8), 7.48–7.32 (m, 5H, Ph), 5.37 (s, 2H, major, CH₂CON), 5.18 (s, 2H, minor, CH₂CON), 5.23 (s, 2H, PhCH₂), 4.35 (s, 2H, minor, CH₂COOH), 3.99 (s, 2H, major, CH₂COOH), 3.54–3.02 (m, CH₂CH₂), 2.93 (s, 3H, major, BocNCH₃), 2.84 (s, 3H, minor, BocNCH₃), 1.39 (s, 9H, *t*-Bu); FAB-MS: *m/z* 542 (M⁺ + H); Calc. for C₂₅H₃₁N₇O₇: C, 55.44; H, 5.77; N, 18.10. Found: C, 55.10; H, 5.71; N, 17.81%.

***N*-{2-[(*N*-*tert*-Butyloxycarbonyl)-*N*-methyl]aminoethyl}-*N*-{[6-*N*-(benzyloxycarbonyl)guanin-9-yl]acetyl}glycine 6d.** To a solution of 5d (2.33 g, 4.0 mmol) in MeOH (40 ml) was added 2 M aqueous NaOH (40 ml). After 1 h at room temperature the reaction mixture was cooled to 0 °C and the pH was adjusted to 2 using 2 M aqueous HCl. The precipitate was filtered, dried and recrystallised from absolute EtOH yielding 1.27 g (43%) of a white solid; mp 189–192 °C; ¹H NMR (400 MHz, DMSO-*d*₆): δ 11.42 (broad, 1H, COOH), 7.92 (s, 1H, major, G-H8), 7.85 (s, 1H, minor, G-H8), 7.55–7.38 (m, 5H, Ph), 5.33 (s, 2H, PhCH₂), 5.18 (s, 2H, major, CH₂CON), 5.00 (s, 2H, minor, CH₂CON), 4.32 (s, 2H, minor, CH₂COOH), 4.05 (s, 2H, major, CH₂COOH), 3.62–3.30 (m, CH₂CH₂), 2.95 (s, 3H, major, BocNCH₃), 2.82 (s, 3H, minor, BocNCH₃), 1.38 (s, 9H, *t*-Bu); FAB-MS: *m/z* 558 (M⁺ + H); Calc. for C₂₅H₃₁N₇O₈: C, 53.86; H, 5.60; N, 17.59. Found: C, 53.54; H, 5.54; N, 17.30%.

Synthesis of PNA oligomers

Coupling of the monomers was carried out according to published protocols³¹ using a 4-(methylbenzhydryl)amine resin down-loaded to 0.12 mmol g⁻¹ with Boc-L-lysine(2-Cl-Z)OH. The PNAs were cleaved from the resin using a trifluoromethanesulfonic acid (TFMSA)–TFA procedure.³¹ Syntheses typically gave a crude product of greater than 90% purity as judged by reversed-phase HPLC. The oligomers were purified by HPLC and characterised by MALDI-TOF mass spectrometry.

Crystallization of H-C_{Me}GT_{Me}AC_{Me}G-(L-Lys)-NH₂

A 5 mg ml⁻¹ solution of self-complementary *N*-methylated PNA [H-C_{Me}GT_{Me}AC_{Me}G-(L-Lys)-NH₂] was screened for crystallization conditions using the sparse-matrix screen of Jancarik and Kim³² from Hampton Research. Optimization of initial crystallization conditions resulted in crystals of size 0.600 × 0.250 × 0.075 mm. The hanging-drop vapor-diffusion method was used at room temperature with drop sizes of 5 μl (3 μl *N*-methylated PNA solution and 2 μl well solution) and 0.5 ml of well solution. The well solution contained 0.4 M MgCl₂, 5% ethanol, 0.075 M TRIS·HCl pH 7.2, and 3.0 M hexane-1,6-diol. *N*-Methylated PNA crystallizes in space group *P*2₁ with cell dimensions *a* = 48.94, *b* = 31.00, *c* = 50.74 Å, β = 111.78°.

Table 1 Diffraction data and refinement statistics

Diffraction data		
Resolution/Å ²	25.0–2.2	(2.24–2.20)
Unique reflections	6794	
Completeness (%)	92.0	(93.0)
Multiplicity	1.6	
$R_{\text{merge}}(I)^a$ (%)	7.5	(30.0)
$1/\sigma I$	6.6	(2.2)
Refinement		
Resolution/Å	6.0–2.2	
Number of reflections	4049	
σ cut-off	3	
R -value/ R_{free} -value ^b (%)	21.4/29.4	
Total number of non-hydrogen atoms	1343	
Water molecules	207	
Average B -values of PNA units/Å ²	19	
Average B -values of L-Lys units/Å ²	51	
Average B -values of water molecules/Å ²	41	
R.m.s. deviation of bond lengths/Å ²	0.015	
R.m.s. deviation of bond angles/°	3.7	

^a R_{merge} = agreement between symmetry related reflections. ^b R_{free} = cross-validation R -value for test set of reflections (10%) omitted during the refinements.

Crystallography

Data collection. A diffraction data set of *N*-methylated PNA was collected to 2.2 Å resolution using one crystal on a Rigaku RU-200 rotating-anode generator equipped with an R-Axis II imaging plate detector ($\lambda = 1.542$ Å, 50 kV, 180 mA, normal focus). The data collection was performed at room temperature with a crystal–detector distance of 100 mm and with 180° rotation in steps of 3° oscillations. Autoindexing and data processing were performed with DENZO³³ and the CCP4 suite of programs.³⁴ The statistics of the data set are tabulated in Table 1.

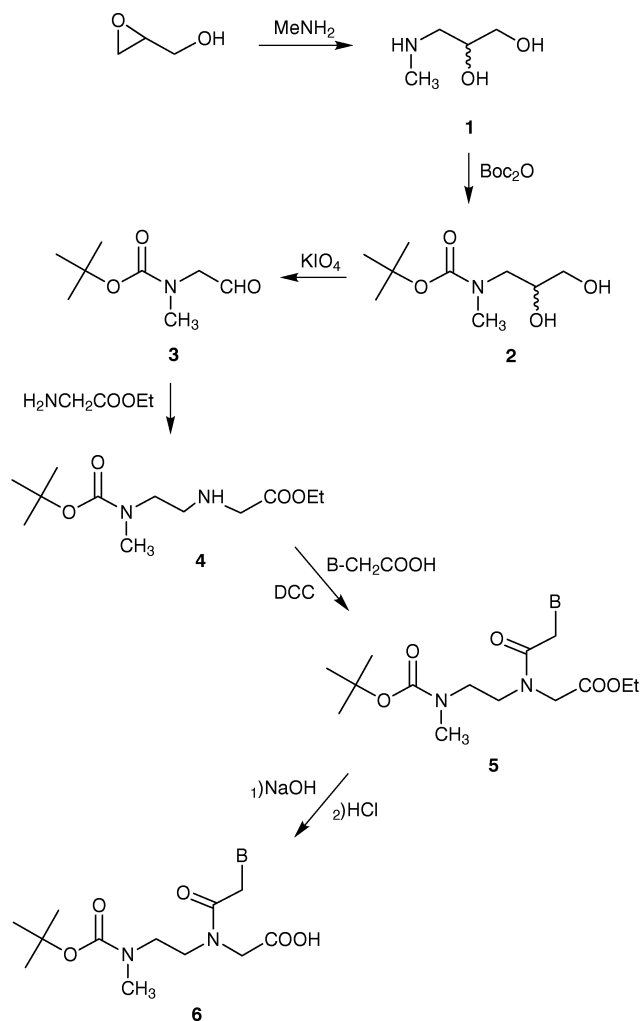
Structure determination and refinement. The structure of *N*-methylated PNA was solved by molecular replacement using the program AMoRe³⁵ from CCP4. Two right-handed and two left-handed double helices have been located per asymmetric unit. The two right-handed and the two left-handed helices, respectively, are related by a translation of 0.50, 0.50, 0.15, as indicated in a native Patterson map. Initially, a right-handed double helix, coaxially stacked with a left-handed helix, of an unmodified PNA-PNA hexamer was used as search model³⁰ in the resolution range 10.0–3.0 Å. One clear solution to the translation function appeared with the best solution from the rotation search. A second translation search was conducted, fixing the first solution to the translation function. After each translational search, ten cycles of rigid-body refinement were performed using AMoRe, resulting in R factors of 56.3% and 52.7%, respectively, and correlation coefficients of 64.4 and 72.3.

The four double helices were subjected to a positional refinement protocol in X-PLOR³⁶ using data in the resolution range 6.0–2.2 Å and a 3σ cut-off, alternating with graphical sessions using the program O.³⁷ Non-crystallographic symmetry restraints were applied during refinement. B -Factor refinement and water molecules were included in the early cycles of refinement. The final R -value was 21.4% and the final refinement statistics and average B -values are tabulated in Table 1. The atomic coordinates of *N*-methylated PNA have been deposited in the Brookhaven Protein Data Bank, accession code RCSB009127.

Results and discussion

Synthesis of *N*-methyl monomers and oligomerization

Monomers suitable for incorporation using Boc-based peptide synthesis were prepared according to Scheme 1. Essentially the chemistry was adapted from existing chemistry used to



Scheme 1 B = a thymine, b *N*⁴-benzyloxycarbonylcytosine, c *N*⁶-benzyloxycarbonyladenine, d *N*²-benzyloxycarbonylguanine.

construct the regular PNA monomers.^{31,38,39} Reaction of aqueous methylamine with 2,3-epoxypropanol produced **1** which after Boc protection of the amine was oxidatively cleaved with KIO_4 to produce **3**. The backbone **4** was obtained from reductive alkylation of ethyl glycinate with **3**. The nucleobase acetic acids were synthesised as described in the literature.³⁸ Coupling of the four nucleobase acetic acids using DCC–DhbtOH followed by alkaline hydrolysis yielded the four monomers **6a–d**.

Duplex formation and stability

Decamer PNA oligomers of mixed pyrimidine–purine content were used for studies of duplex formation with complementary DNA, RNA and PNA oligomers. Two PNAs were synthesised; PNA **I** containing three *N*-methyl backbone thymines and PNA **II** in which all monomers derived from the *N*-methyl backbone. Thermal stability studies of the duplexes formed between these PNAs and DNA, RNA or PNA are presented in Table 2. The data clearly demonstrate that inclusion of *N*-methyl backbone units results in a decrease in thermal stability of the PNA-nucleic acid duplexes of 1–3 °C per *N*-methyl unit. It is also observed that the effect is less pronounced for RNA (and PNA) binding and that the effect of having more *N*-methyl units is not “additive”, since the cost per *N*-methyl is higher for PNA **I** than for PNA **II**. Furthermore, we note that even the fully methylated PNA **II** exhibits PNA-nucleic acid duplex stabilities that are equal to (DNA) or significantly higher (RNA) than that of the corresponding DNA oligonucleotide. Finally, it is interesting that the relative

Table 2 Thermal stabilities ($T_m/^\circ\text{C}$) of PNA-DNA, PNA-RNA, PNA-PNA duplexes

PNA-DNA	Anti-parallel DNA duplex ^a	Parallel DNA duplex ^b	Mismatch ^c	RNA ^d	RNA mismatch ^e	PNA ^f
H-GT _{Me} AGAT _{Me} CACT _{Me} -NH ₂ (I)	41.5 (2.8) ^g	37.5	~37 ^h	48.5 (1.8)	39	63.0 (1.3)
H-(GTAGATCACT) _{Me} -LysNH ₂ (II)	33.0 (1.8)	34.5	—	44.0 (1.2)	—	61.5 (0.6)
H-GTAGATCACT-NH ₂ (IIIa)	50	38.5	~40 ^h	54	44	67
H-GTAGATCACT-LysNH ₂ (IIIb)	51	38	~37 ^h	56	46	67
5'-GTAGATCACT-3'	33.5		26.5	34	32	49

^a 5'd(AGTGTACTAC). ^b 5'd(CATCTAGTGA). ^c 5'd(AGTGGTCTAC). ^d 5'(AGUGAUCUAC). ^e 5'(AGUGGUCUAC). ^f H-AGTGTACTAC-LysNH₂. ^g ΔT_m per *N*-methyl unit given in parentheses. ^h Due to a thermal transition of the single stranded PNA itself around 40 °C, this value is difficult to determine accurately.

Table 3 Thermal stabilities ($T_m/^\circ\text{C}$) of (PNA)₂-DNA triplexes

PNA	DNA (ap) ^a	DNA (p) ^b	RNA ^c	PNA ^c
H-T ₁₀ -LysNH ₂ (IV)	71.5 (0) ^d		81	70
H-TTTTTT _{Me} TTTT-LysNH ₂ (V)	66.0 (2.7)			56
H-TTTTTT _{Me} TT _{Me} TTT-LysNH ₂ (VI)	61.5 (2.5)			63.5
H-TTTT _{Me} TT _{Me} TT _{Me} TT-LysNH ₂ (VII)	57.0 (1.5)		58	56.5
H-Gly-(TTTTTTTTT) _{Me} -LysNH ₂ (VIII)	43.0 (1.4)		42	48
H-TJTJTJT(eg) ₃ -TTTCTCT-LysNH ₂ (IX)	64.0 (0)	49		
H-T _{Me} JT _{Me} JT _{Me} T _{Me} T _{Me} (eg) ₃ TTTCTCT-LysNH ₂ (X)	42.0 (4.4)	~39		
H-TJTJTJT(eg) ₃ T _{Me} T _{Me} T _{Me} C _{Me} T _{Me} C _{Me} T _{Me} -LysNH ₂ (XI)	40.5 (3.3)	31		
TJTJTJT(eg) ₃ T _{Me} T _{Me} T _{Me} CT _{Me} CT _{Me} -LysNH ₂ (XII)	48.5 (2.2)	32.5		
TJTJTJT(eg) ₃ TTT _{Me} TC _{Me} T-LysNH ₂ (XIII)	55.5 (4.3)	32		

^a Sequences: 5'd(CGCA₁₀CGC) or 5'd(CGCAGAGAAAACGC), ap: anti-parallel, p: parallel. ^b Sequence 5'd(CGCAAAAGAGACGC). ^c Sequence: A₁₀. ^d ΔT_m per *N*-methyl unit given in parentheses.

preference of PNA for binding to DNA in the antiparallel orientation is diminished (PNA **I**) or completely abolished (PNA **II**) for the *N*-methylated PNAs.

Triplex formation and stability

Two formats were chosen for the study of (PNA)₂-DNA triplexes. The first consisted of a T₁₀ with an increasing number (1, 2, 3 or 10) of *N*-methyl substitutions. The second format was a bis(PNA) in which the *N*-methyl substitutions were made in the Watson-Crick or the Hoogsteen strand, respectively. The results are presented in Table 3. Analogously to what was observed for duplex formation, inclusion of the *N*-methylated PNA backbone decreases the thermal stability of the (PNA)₂-DNA triplexes by an average 2 °C per *N*-methyl unit, and the effect is diminished with an increasing number of *N*-methyl units (compare PNAs **V**–**VIII**). [Using PNA **VII** as a representative case, we performed a titration (Job-plot) to ascertain that indeed (PNA)₂-DNA triplexes are formed by these *N*-methyl substituted PNAs (Fig. 1)]. In order to address whether the effect of the methylation was confined to

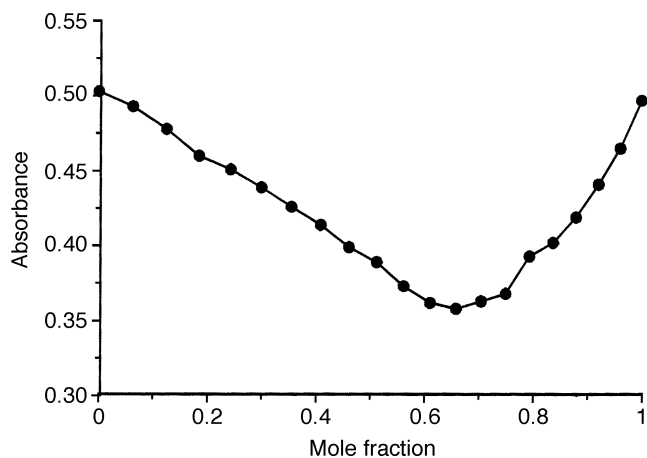


Fig. 1 Titration (Job-plot) of the binding of PNA **VII** to a complementary oligonucleotide (dA₁₀).

the Watson-Crick interaction or was also affecting the Hoogsteen strand, we synthesized a series of linked bis(PNAs) in which the preferred binding mode (Watson-Crick *versus* Hoogsteen) can be controlled by the orientation of the PNA strands (antiparallel orientation is preferred by the Watson-Crick PNA strand whereas parallel orientation is preferred by the Hoogsteen PNA strand), as well as the position of pseudo-isocytosine (J) nucleobases, which do not require low pH for optimal J-G Hoogsteen type interactions.⁴⁰ Thus for the triplexes of PNAs **IX**–**XIII** presented in Table 3, Hoogsteen binding should be preferred by the “J-strand”, while Watson-Crick binding should take place with the “C-strand”. This assignment is supported by the fact that all of these PNAs bind more strongly to the DNA complement that is antiparallel to the PNA “C-strand” than to the DNA complement that is parallel to this strand (Table 3). Therefore by comparing the result obtained with PNA **X** having five (thymine) *N*-methyl units in the Hoogsteen strand ($\Delta T_m = 4.4^\circ\text{C}$) with that of PNA **XII** having five (thymine) *N*-methyl units in the Watson-Crick strand ($\Delta T_m = 2.2^\circ\text{C}$) we conclude that *N*-methylation affects the stability of both strands, and that the interference seems greater in the Hoogsteen strand.

CD spectroscopy

We applied circular dichroism spectroscopy to monitor any effects of the backbone *N*-methylation on the structure of the PNA-nucleic acid complexes. The results presented in Fig. 2 and 3 clearly show that no major structural change occurs in the PNA-DNA or PNA-RNA duplexes or (PNA)₂-DNA triplexes upon introduction of 30% (three out of ten) *N*-methyl units in the PNA strand(s). However, most interestingly, the complexes (duplex or triplex) formed by the fully methylated PNAs **II** and **VIII** show distinctly altered CD spectra, strongly suggesting that these complexes also have structures that distinguish them from those formed by the normal PNAs. On the other hand no major difference between the PNA-PNA duplexes formed by the fully methylated PNA **II** as compared to that of the normal PNA **I** was apparent from CD spectroscopy (Fig. 4).

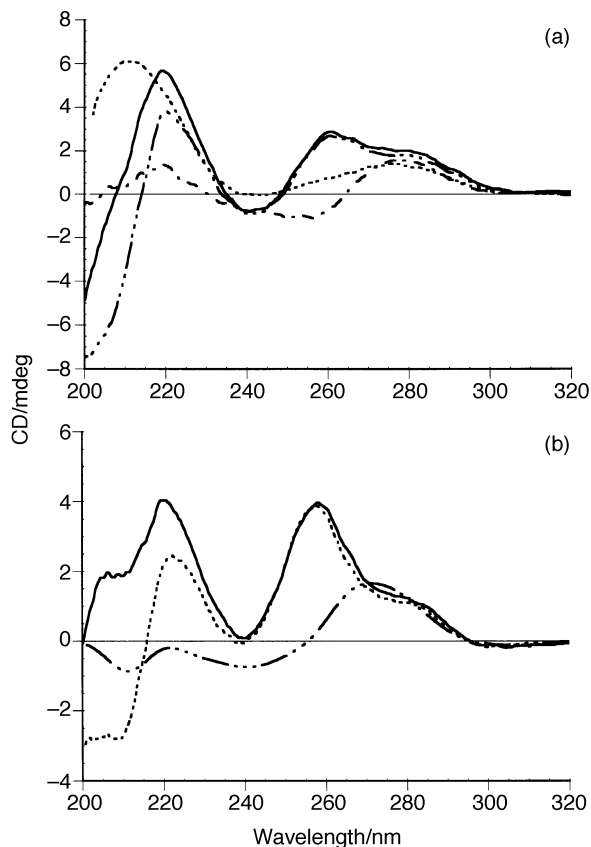


Fig. 2 Circular dichroism (CD) spectra of the duplexes between PNAs I (—), II (---) or the control PNA IIIa (— · —) and the antiparallel DNA (a) or RNA (b) oligonucleotide (5'-AGTGATCTAC). CD spectra of the free DNA or RNA are shown by (— · —).

This is also consistent with the observation that *N*-methyl backbone substitutions are more easily accommodated in PNA-PNA duplexes ($\Delta T_m \approx 0.6\text{--}1.3^\circ\text{C}$ per *N*-methyl substitution) than in PNA-DNA (RNA) duplexes ($\Delta T_m 1.2\text{--}2.8^\circ\text{C}$ per substitution). It has been shown that a PNA-PNA duplex adopts a novel helical conformation, the P-form³⁰ that shows a much larger helical pitch (≈ 18 bases per turn) and diameter (≈ 28 Å) than the natural B- or A-form conformations which are closer to the structures adopted by PNA-DNA and PNA-RNA duplexes.^{27,28} Thus it appears that the *N*-methyl PNA backbone can be quite easily accommodated in the P-type helix, whereas it is more difficult in the B- or A-type helices.

The (PNA)₂-DNA triplexes also adopt a P-type conformation,²⁹ but nonetheless do not seem to accommodate the *N*-

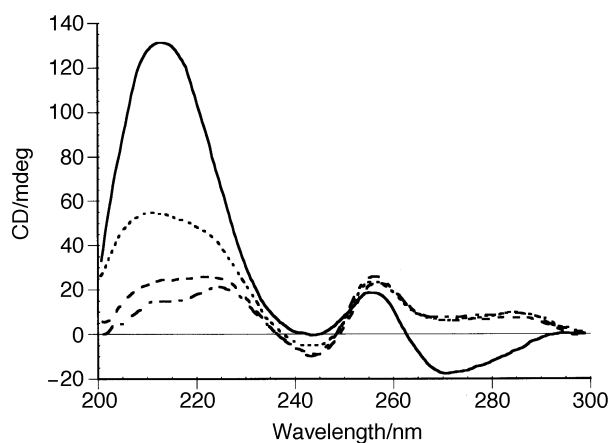


Fig. 3 CD spectra of the triplexes between dA₁₀ and T₁₀ PNAs IV (control) (—), V (one *N*-methyl) (---), VII (three *N*-methyl) (--- · ---), and VIII (full *N*-methyl) (— · —).

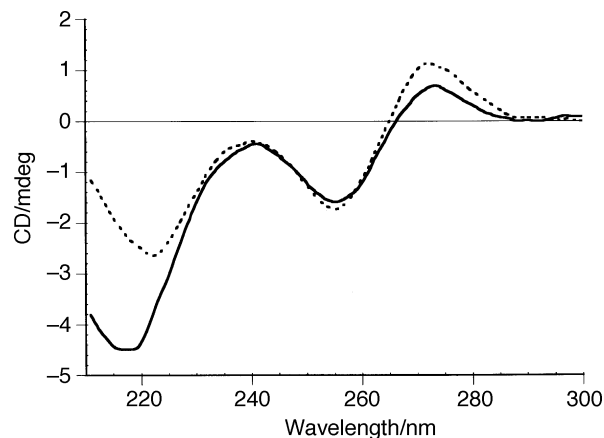


Fig. 4 CD spectra of the duplexes formed between PNA II (—) or the control PNA I (---) and a complementary PNA (having a C-terminal L-lysine).

methyl backbone any better than PNA-DNA (RNA) duplexes. Furthermore, the largest effect is seen when the *N*-methyl backbone is placed in the Hoogsteen strand (compare PNAs X and XIII). This is most likely due to disruption of N-H...phosphate hydrogen bonding interactions between the backbone of the DNA and the Hoogsteen PNA strand as observed in the crystal structure and suggested to provide extra stabilization of the (PNA)₂-DNA triplex.²⁹

Crystal structure determination

The structure of a 50% *N*-methylated PNA hexamer [H-C_{Me}GT_{Me}AC_{Me}G(L-Lys)-NH₂] was determined in order to establish how the *N*-methyl backbone is accommodated in the P-type helix of PNA-PNA duplexes. The asymmetric unit of the crystal contains two pairs of coaxially stacked right-handed and left-handed double helices (Fig. 5). As previously observed,³⁰ this results, by crystallographic symmetry, in the formation of a continuous pseudo-helix, alternating between right- and left-handed forms. The two right-handed and the two left-handed helices are very similar. The *N*-methylated PNA hexamer adopts the P-form helix (Table 4) with helical parameters close to those of the unmodified PNA-PNA duplex.³⁰

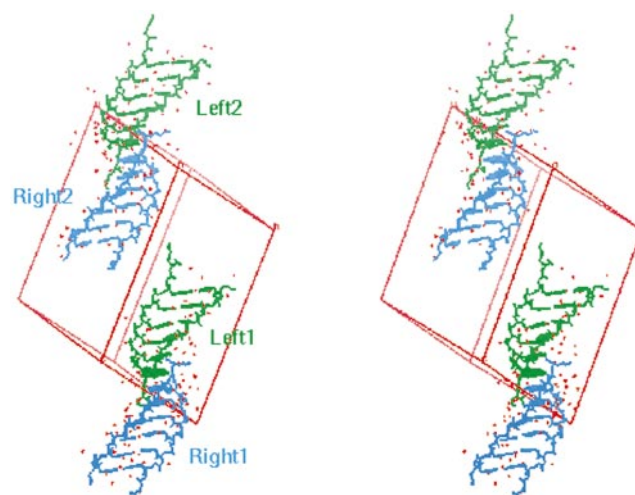


Fig. 5 The *N*-methylated PNA hexamer crystallizes with two right-handed (cyan) and two left-handed (green) double helices in the asymmetric unit. The right-handed and left-handed helices are coaxially stacked. The two right-handed and the two left-handed helices, respectively, are related by non-crystallographic translational symmetry. The unit cell with axes is shown in stereo. The figure was generated using the program O.³⁷

Table 4 Helical parameters (average)^a of the *N*-methylated PNA-PNA duplex

	Twist (%)	Rise/Å	Base tilt (%)	Displacement/Å	Bases per turn
N-Me PNA ^b					
Right1	18.9	3.8	0.2	4.8	18
Right2	19	3.8	0.1	4.9	18
Left1	-20	3.5	0	7.2	18
Left2	-20	3.5	0.3	7.2	18
Unmodified PNA ^c	19.8	3.2	1	8.3	18

^a The helical parameters were determined using the program CURVES.⁴¹ ^b N-Me PNA: backbone *N*-methylated PNA-PNA duplex [H-C_MGT_MAC_MG-(L-Lys)-NH₂]. ^c Unmodified PNA: unmodified PNA-PNA duplex (H-CGTACG-NH₂).³⁰

The major structural difference between *N*-methylated and unmodified PNA is an alteration in the conformation of the *N*-methyl substituted amide moiety. In the *N*-methylated PNA, the backbone carbonyl oxygens of the affected amide moieties are turned inward towards the nucleobases (Fig. 6) whereas the carbonyl oxygens are directed into solution in the structure of unmodified PNA.³⁰ In the structure of the unmodified PNA hexamer specific water molecules that form a bridge between the backbone amide NH and the nucleobase were located for each base step. This hydrogen bonding donor has been eliminated in the modified PNA backbone. However, the water bridge is retained by coordination of the carbonyl oxygen and the water molecule, thereby leaving the *N*-methyl moiety exposed to the solvent. The water bridge between the backbone amide NH and the nucleobase is retained in the unmodified amide moieties of the *N*-methylated PNA, either through backbone amide NH or through the carbonyl oxygen, as two of these non-methylated amide moieties in each strand adopt two different conformations.

The backbone–nucleobase interactions through water molecules seem important for stabilizing the P-form helix of PNA. These interactions are still possible within the modified PNA backbone, and probably explain why no major overall structural difference is apparent between the PNA-PNA duplexes formed by *N*-methylated PNA as compared to normal PNA.

Conclusion

The present results demonstrate that PNA duplex (with DNA, RNA or PNA) and to a lesser extent (PNA)₂-DNA triplex

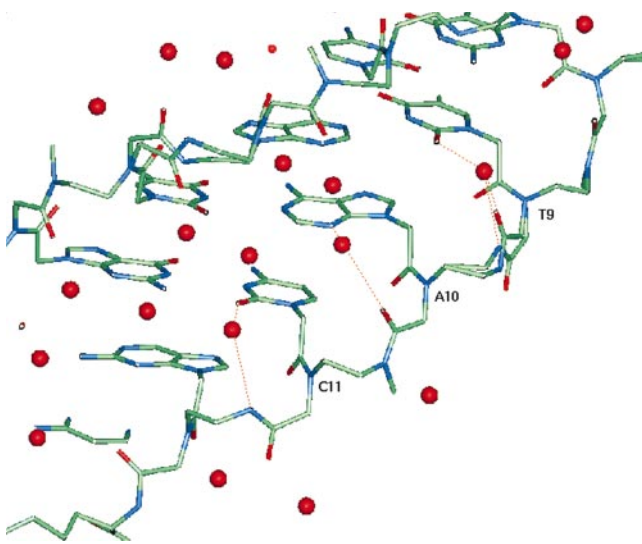


Fig. 6 Backbone (amide NH or O) forms hydrogen bonds to water molecules, bridging the nucleobase and backbone in the double helical structure of the methylated PNA-PNA hexamer. Three representative base pairs are shown. PNA is colored by atom-types, and water molecules are depicted as red spheres. The figure was generated using the program O.³⁷

structures can without major loss in stability accommodate a limited number (at least 30%) of *N*-methyl substitutions in the backbone. Most interestingly, duplexes and triplexes with fully methylated PNAs adopt helix conformations which judged by CD are distinctly different from the regular PNA structures. The crystal structure of the 50% modified PNA-PNA duplex shows that the *N*-methyl group is accommodated in the double helical structure by an alteration in the conformation of the affected amide moiety. This clearly indicates that NH hydrogen bonding is not crucial for stabilization of the structure as long as the possibility for formation of a nucleobase–backbone bridge through a water molecule is present. In conclusion these results indicate that *N*-alkylation can with only a moderate loss of hybridization potency be exploited as a means to modulate, for example the pharmacological properties of PNA.

Acknowledgements

The technical assistance of Annette Jørgensen and Brian Rosenberg is gratefully acknowledged. The work was supported by grants from The Danish National Research Foundation, PharmaBiotec and The Lundbeck Foundation.

References

- 1 E. Uhlmann and A. Peyman, *Chem. Rev.*, 1990, **90**, 544.
- 2 A. De Mesmaeker, K. H. Altmann, A. Waldner and S. Wendeborn, *Curr. Opin. Struct. Biol.*, 1996, **5**, 343.
- 3 M. Matteucci and R. W. Wagner, *Science*, 1996, **384**, suppl. 20.
- 4 P. E. Nielsen, M. Egholm, R. H. Berg and O. Buchardt, *Science*, 1991, **254**, 1497.
- 5 M. Egholm, O. Buchardt, P. E. Nielsen and R. H. Berg, *J. Am. Chem. Soc.*, 1992, **114**, 1895.
- 6 B. Hyrup and P. E. Nielsen, *Bioorg. Biomed. Chem.*, 1996, **4**, 53.
- 7 M. Eriksson and P. E. Nielsen, *Quart. Rev. Biophysics*, 1996, **29**, 369.
- 8 H. Knudsen and P. E. Nielsen, *Anti Cancer Drugs*, 1996, **8**, 113.
- 9 P. E. Nielsen and G. Haaiima, *Chem. Soc. Rev.*, 1997, **26**, 73.
- 10 L. Good and P. E. Nielsen, *Antisense Nucleic Acid Drug Dev.*, 1997, **7**, 431.
- 11 E. Uhlmann, A. Peyman, G. Breipohl and D. W. Will, *Angew. Chem., Int. Ed.*, 1998, **37**, 2796.
- 12 G. Haaiima, A. Lohse, O. Buchardt and P. E. Nielsen, *Angew. Chem., Int. Ed. Engl.*, 1996, **35**, 1939.
- 13 A. Lenzi, G. Reginato and M. Taddei, *Tetrahedron Lett.*, 1995, **36**, 1713.
- 14 E. Lioy and H. Kessler, *Liebigs Ann.*, 1996, 201.
- 15 A. H. Krotz, O. Buchardt and P. E. Nielsen, *Tetrahedron Lett.*, 1995, **36**, 6937.
- 16 A. H. Krotz, O. Buchardt and P. E. Nielsen, *Tetrahedron Lett.*, 1995, **36**, 6941.
- 17 B. Hyrup, M. Egholm, O. Buchardt and P. E. Nielsen, *Bioorg. Med. Chem. Lett.*, 1996, **6**, 1083.
- 18 P. Lagriffoule, O. Buchardt, P. Wittung, B. Nordén, K. K. Jensen and P. E. Nielsen, *Chem. Eur. J.*, 1997, **3**, 912.

- 19 S. Jordan, C. Schwemler, W. Kosch, A. Kretschmer, U. Stropp, E. Schwenner and B. Mielke, *Bioorg. Med. Chem. Lett.*, 1997, **7**, 687.
- 20 A. Peyman, E. Uhlmann, K. Wagner, S. Augustin, G. Breipohl, D. W. Will, A. Schäfer and H. Wallmeier, *Angew. Chem., Int. Ed. Engl.*, 1996, **35**, 2636.
- 21 N. M. Howarth and L. P. G. Wakelin, *J. Org. Chem.*, 1997, **62**, 5441.
- 22 C. Garcia-Escheverria, D. Hüsken, C. S. Chiesi and K.-H. Altmann, *Bioorg. Med. Chem. Lett.*, 1997, **7**, 1123.
- 23 V. S. Rana, V. A. Kumar and K. N. Ganesh, *Bioorg. Med. Chem. Lett.*, 1997, **7**, 2837.
- 24 V. A. Efimov, M. V. Choob, A. A. Buryakova, A. L. Kalinkina and O. G. Chakhmakheva, *Nucleic Acids Res.*, 1998, **26**, 566.
- 25 Ö. Almarsson, T. C. Bruice, J. Kerr and R. N. Zuckermann, *Proc. Natl. Acad. Sci. USA*, 1993, **90**, 7518.
- 26 Ö. Almarsson and T. C. Bruice, *Proc. Natl. Acad. Sci. USA*, 1993, **90**, 9542.
- 27 S. C. Brown, S. A. Thomson, J. M. Veal and D. G. Davis, *Science*, 1994, **265**, 777.
- 28 M. Eriksson and P. E. Nielsen, *Natur. Struct. Biol.*, 1996, **3**, 410.
- 29 L. Betts, J. A. Josey, J. M. Veal and S. R. Jordan, *Science*, 1995, **270**, 1838.
- 30 H. Rasmussen, J. S. Kastrup, J. N. Nielsen, J. M. Nielsen and P. E. Nielsen, *Natur. Struct. Biol.*, 1996, **2**, 98.
- 31 L. Christensen, R. Fitzpatrick, B. Gildea, K. H. Petersen, H. F. Hansen, T. Koch, M. Egholm, O. Buchardt, P. E. Nielsen, J. Coull and R. H. Berg, *J. Pept. Sci.*, 1995, **3**, 175.
- 32 J. Jancarik and S.-H. Kim, *J. Appl. Crystallogr.*, 1991, **24**, 409.
- 33 Z. Otwinowski, in *Proceedings of the CCP4 Study Weekend: Data Collection and Processing*, ed. L. Sawyer, N. Isaacs and S. S. Bailey, SERC Daresbury Laboratory, Warrington, 1993, pp. 56–62.
- 34 Collaborative Computational Project, Number 4, *Acta Crystallogr., Sect. D*, 1994, **50**, 760.
- 35 J. Navaza, *Acta Crystallogr.*, 1994, **50**, 157.
- 36 T. A. Brünger, J. Kuriyan and M. Karplus, *Science*, 1987, **235**, 458.
- 37 T. A. Jones, J.-Y. Zou, S. W. Cowan and M. Kjeldgaard, *Acta Crystallogr., Sect. A*, 1991, **47**, 110.
- 38 K. L. Dueholm, M. Egholm, C. Behrens, L. Christensen, H. F. Hansen, T. Vulpius, K. Petersen, R. H. Berg, P. E. Nielsen and O. Buchardt, *J. Org. Chem.*, 1994, **59**, 5767.
- 39 K. L. Dueholm and P. E. Nielsen, *New J. Chem.*, 1997, **21**, 19.
- 40 M. Egholm, L. Christensen, K. L. Dueholm, O. Buchardt, J. Coull and P. E. Nielsen, *Nucleic Acids Res.*, 1995, **23**, 217.
- 41 R. Lavery and H. J. Sklenar, *J. Biomol. Struct. Dyn.*, 1998, **6**, 63.

Paper 9/02091H